Scripta Materialia 149 (2018) 134–138

Contents lists available at ScienceDirect

Scripta Materialia

journal homepage: www.elsevier.com/locate/scriptamat

Regular article

Origin of enhanced piezoelectric properties and room temperature multiferroism in MnO_2 added $0.90(Li_{0.12}Na_{0.88}NbO_3)$-$0.10BaTiO_3$ ceramic

Supratim Mitra [a,*], T. Karthik [b], Jayant Kolte [c], Ramesh Ade [b], N. Venkataramani [b], Ajit R. Kulkarni [b]

[a] Department of Physics, Banasthali Vidyapith, Banasthali-304022, Rajasthan, India
[b] Department of Metallurgical Engineering and Materials Science, Indian Institute of Technology Bombay, Mumbai 400 076, Maharashtra, India
[c] School of Physics and Materials Science, Thapar Institute of Engineering and Technology, Patiala 147004, Punjab, India

ARTICLE INFO

Article history:
Received 29 December 2017
Accepted 15 February 2018

Keywords:
Piezoelectric ceramics
Ferroelectricity
Piezoelectricity
Magnetic properties

ABSTRACT

Room temperature multiferroism with enhanced ferro and piezoelectric properties of a new lead-free MnO_2 added $0.90(Li_{0.12}Na_{0.88}NbO_3)$-$0.10BaTiO_3$ ceramic is reported. The addition of MnO_2 as an additive resulted in a two fold increase in remnant polarization (P_r) (from ~7.30 to 17.20 μC/cm^2), ~50% increase in large-signal piezoelectric coefficient (d^*_{33}) (from ~117 to176 pm/V) and symmetric butterfly loop are observed. Phase analysis revealed that MnO_2 entered the host lattice as Mn^{2+} and Mn^{4+}-ions and induced room temperature ferromagnetic-like character. Interestingly, an intrinsic coupling between the two ferroic orders is evidenced by the observation of a magneto-electric voltage coefficient (α_E) of ~0.94 mV/cm.Oe.

Development of lead-free ferro/piezoelectric materials with properties on par with lead-based materials has created significant interest in the scientific/technological community [1]. The focus on lead-free ferro/piezoelectrics has been based on the modified alkali bismuth titanates [2], alkali niobates [3], and other systems with morphotropic phase boundaries (MPB) [1,4]. In our recently reported work, a new lead-free $(100–x)Li_{0.12}Na_{0.88}NbO_3 - xBaTiO_3 (0 < x < 40)$ piezoelectric ceramic with a morphotropic phase boundary (MPB) composition in the range between $x = 0.10–0.12$ has been synthesized [5,6]. The MPB compositions between LNN ($La_{0.12}Na_{0.88}NbO_3$) and BT ($BaTiO_3$) exhibited high Curie temperature (>250 °C), high relative density (>97%), enhancement in remnant polarization (P_r), improved large and small signal piezoelectric coefficients (d^*_{33} & d_{33}) and quality factor (Q_m) [6]. Though a noticeable enhancement in the properties was achieved in LNN-BT solid solutions, asymmetry in the butterfly-loop and non-squared ferroelectric hysteresis loop has been found as a drawback which could restrict this material for various actuating and sensing applications [1]. Therefore, in order to utilize these high-performance lead-free materials in final industrial applications, the aforementioned drawbacks have to be resolved along with further enhancement of the ferro and piezoelectric properties. In this regard, several approaches such as site-specific substitution [7], addition of transition metal oxides or rare earth oxides as additives [8] and modified processing routes [9–11] have been adopted to enhance the piezoelectric properties. Amongst these, addition of oxides as an additive provide a simple way to influence the piezoelectric properties. MnO_2 is one such additive commonly used for enhancing the piezoelectric properties [12–14]. In view of this, we have chosen a composition near the MPB region, i.e., 0.90(LNN)-0.10(BT) and 1 mol% $MnO_2$was added to it. The choice of 1 mol% MnO_2 among the various concentrations of MnO_2 was based on significant enhancement in ferro, piezo and electrical properties, and would be reported separately. Apart from enhanced piezo and ferroelectric properties, MnO_2 is also known to induce magnetism if it goes into the host lattice or even if it resides on the surface as the parasitic phase at the grain boundaries as observed in $SrTiO_3$ and $KTaO_3$ systems [15,16]. In order to achieve intrinsic coupling between the multiferroic order parameters, the additives should occupy the host lattice. Thus, inducing magnetism intrinsically in LNNBT through addition of MnO_2 may lead to exhibit multiferroic properties and realize applications in novel electronic devices [17,18]. Multiferroic properties have been observed in several non-magnetic ferro/piezoelectric perovskites when magnetically active transition metal cations such as Mn, Fe, Ni and Co have been site-specifically substituted at the B-site of the perovskite system [15,16,19–23]. Though room temperature multiferroism is reported in such single-phase systems, the magneto-electric (ME) coupling is reported only in a few systems. From an application perspective, sizeable room temperature ME response with good ferro and piezoelectric properties are highly desirable. Thus, in this work, we have reported a very interesting room temperature multiferroism and magneto-electric coupling in a single phase system with enhanced properties by a simple MnO_2 addition to LNNBT system.

The phase formed $0.90(Li_{0.12}Na_{0.88}NbO_3)$-$0.10BaTiO_3$ ceramic powders (labeled as LNNBT) were synthesized from the high purity

* Corresponding author.
E-mail address: supratimmitra2003@gmail.com (S. Mitra).

https://doi.org/10.1016/j.scriptamat.2018.02.020
1359-6462/

(~99.9%) raw materials viz., Nb_2O_5, Na_2CO_3, Li_2CO_3, TiO_2, and Ba_2CO_3. The detailed synthesis processes for LNN($Li_{0.12}Na_{0.88}NbO_3$) and BT ($BaTiO_3$) were described in Supplementary materials[#] [5,6]. Along with LNNBT, 1 mol% of MnO_2 (labeled as LNNBT:Mn) was added as an additive. The green compacted pellets were sintered at 1150 °C for 3 h in air atmosphere[#]. The phase purity of the sample was checked using X-ray diffractometer (X'Pert, PANalytical). Microstructure and elemental mapping were performed using field emission scanning electron microscopy (FE-SEM) (JEOL JSM-7600F). Dielectric measurements were done using an impedance analyzer (Alpha High Resolution, Novocontrol, Germany) in the temperature range 50 to 500 °C. Polarization (P) vs. electric field (E) hysteresis loops and strain S-E curves were traced using a ferroelectric analyzer (TF Analyzer 2000, aixACCT, Germany) at 1 Hz. Magnetization (M) measurements were performed on a PPMS-VSM (Quantum Design, USA). The X-band (9.2 GHz) electron spin resonance (ESR) experiments were carried out on a JES - FA200 spectrometer (JEOL, Japan). Magnetoelectric (ME) voltage coefficient (α_E) was measured on poled specimens using SR-830 DSP lock-in amplifier [24]. Magneto-dielectric properties were measured by varying DC magnetic field upto 6.5 kOe using an impedance analyzer (Alpha High Resolution, Novocontrol, Germany) and an electromagnet. A similar sample thickness of both LNNBT and LNNBT:Mn was used for all electrical measurements.

Fig. 1(a) shows the XRD patterns of sintered LNNBT and LNNBT:Mn specimens. The observed Bragg reflections confirm a major single phase perovskite structure with orthorhombic symmetry (SG: *Pbma*), characterized by splitting of (202)/(080) peaks for both LNNBT [5] and LNNBT:Mn ceramics. However, a minor secondary $Ba_6Ti_2Nb_8O_{30}$ phase was also observed in both the samples. A closer look at the peaks near $2\theta = 32$ and 46° does not show any shift in their position in LNNBT and LNNBT:Mn confirming no changes in the lattice constant. The results indicate that the addition of very small amount of MnO_2 does not change the crystalline structure within the limit of 1 mol% and MnO_2 can be completely dissolved into the host lattice of LNNBT [12]. In general, Mn ions occupy B-site in the perovskite structure. However, it is hard to choose that A-site cation vacancies or oxygen vacancies will be produced following to the substitution of Mn ions for Nb^{5+}/Ti^{4+} as Mn ions may have distinctive valences after sintering in the air. The role of Mn ions is significant as it will have different effects on the electrical properties as an acceptor or donor dopant. The FE-SEM micrograph of LNNBT:Mn shows densely packed grains (See Fig. 1(b)). The inset of Fig. 1(b) shows the photograph of as-sintered LNNBT and LNNBT:Mn depicting a clear variation in the specimen color upon Mn-substitution. Fig. 1(c) shows the backscattered electron micrograph, which does not show any phase segregation at the grain boundaries. Mn-elemental mapping performed in a selected region (See Fig. 1(c)) within a grain shows that Mn distribution is microscopically homogenous.

Ferroelectric hysteresis loops clearly revealed more than two-fold increase in the remnant polarization (P_r) from ~7.3 to17.2 μC/cm^2 along with a slight increase in the coercive field (E_C) from ~22.3 to 27.5 kV/cm upon Mn substitution in LNNBT (See Fig. 2(a)). The observation of well saturated polarization (P) versus electric field (E), P-E curves indicate the intrinsic ferroelectric character in both LNNBT and LNNBT:Mn specimen [7]. The % strain value (i.e., both bipolar and unipolar strain) increases significantly in LNNBT:Mn as shown in Fig. 2(b) & (c). In addition, the bipolar strain (S) versus electric field (E), S-E curves become more symmetric in the case of LNNBT:Mn (See Fig. 2(b)). The calculated large-signal piezoelectric coefficient (d^*_{33}) shows ~50% increment in LNNBT:Mn i.e., from ~117 pm/V to ~176 pm/V. The ferro and piezoelectric measurements clearly reveal that 1 mol% of MnO_2 addition in LNNBT significantly enhances the P_r, d^*_{33} values. Fig. 2(d) shows temperature (T) dependence of the real part of the dielectric constant (ε') measured at a frequency of 1 kHz for both the specimens. In LNNBT, Curie temperature (T_C) is observed at ~270 °C, whereas in LNNBT:Mn T_C decreases to ~230 °C. In LNNBT:Mn ceramics, the decrease in T_C towards the low temperature side and reduced permittivity could be explained by the following way: The Mn^{2+} (ionic radius for coordination number 6 (IR) = 0.67 Å) ion can possibly replace Nb^{5+} (IR = 0.64 Å)/ Ti^{4+}(IR = 0.605 Å) leaving a less rattling space in the oxygen-octahedra for spontaneous polarization and thereby reduced permittivity at T_C is observed. If, Mn^{4+}(IR = 0.53 Å) would have replaced Nb^{5+}/Ti^{4+} then the rattling space in the oxygen-octahedra would have been larger with higher permittivity value. This result confirms the existence of Mn in the 2+ valence state and an indication of entering into the host lattice. However, the distortion in oxygen-octahedra due to incorporation of Mn is not very significant and therefore no peak shift has been observed in XRD pattern and no superlattice reflections.

In order to understand the effect of Mn-substitution, temperature dependent complex impedance spectra are recorded in the range from 250 to 450 °C for both the specimens. From the complex impedance spectra, grain resistance (R_g) and grain boundary resistance (R_{gb}) values are estimated by fitting these plots using two parallel RC equivalent circuits (See inset of Fig. 2(g)). The activation energies due to grain (E_g) and grain boundary (E_{gb}) calculated using the Arrhenius equation are found to be $E_g = 0.73$ eV; $E_{gb} = 0.80$ eV for LNNBT and $E_g = 0.89$ eV; $E_{gb} = 0.96$ eV for LNNBT:Mn. The increase in activation energies in LNNBT:Mn is due to the reduction in mobile oxygen vacancies [25–27]. In addition, the overall dc conductivity (σ_{dc}) is found to be lower in magnitude for LNNBT:Mn ($\sigma_{dc} = 7.59 \times 10^{-7}$ S/cm at 425 °C) as compared to LNNBT ($\sigma_{dc} = 1.28 \times 10^{-6}$ S/cm at 425 °C). Thus, apart

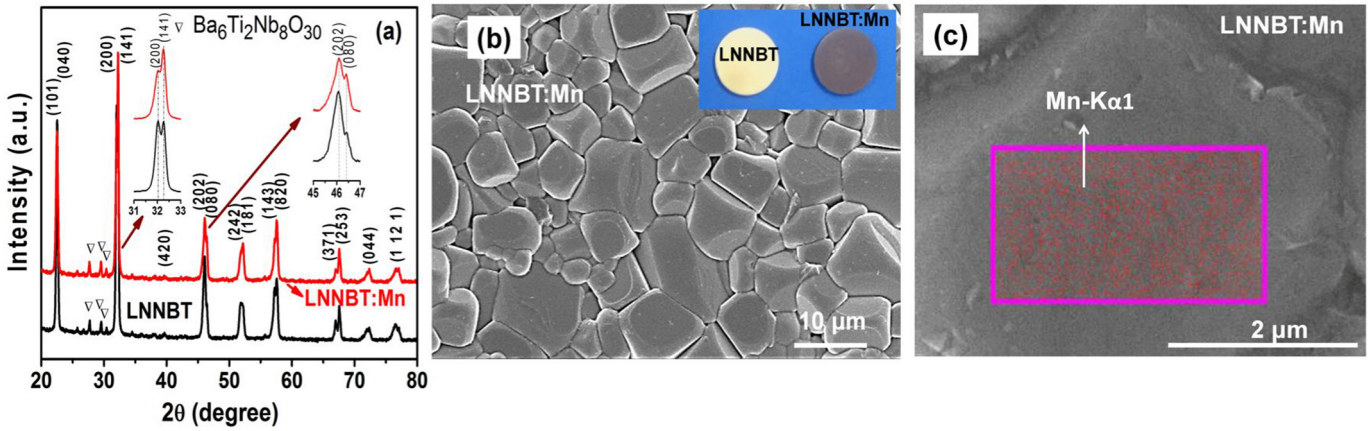

Fig. 1. (a) XRD patterns of sintered LNNBT and LNNBT:Mn specimens along with close observation of Bragg reflections near $2\theta = 32$ and 46 degree (∇-$Ba_6Ti_2Nb_8O_{30}$ secondary phase). (b) Secondary electron micrograph of sintered LNNBT:Mn (*Inset shows the photograph of sintered LNNBT and LNNBT:Mn*), (c) Back scattered electron micrograph of LNNBT:Mn along with Mn elemental mapping in a selected region of a grain.